

HEAT TRANSFER IN EXTRUDER SCREWS

Stephen J. Derezinski, Eastman Kodak Company, Rochester, NY 14652-3701

Abstract

In the study and modeling of the resin temperature in extruder channels, the screw is commonly assumed adiabatic. However, the resin begins as a cold solid and is melted and heated as it flows, which requires that the screw also be cold at the entrance and hot at the exit. Heat must, therefore, be conducted in the screw metal from the hot end of the screw to the cold end, which requires heat transfer with the melt. Also, the heat capacity, especially of larger extruders, can require significant time to attain steady-state operation. A model of transient heat conduction in the screw coupled to heat transfer with the resin feed, melting, and pumping is used to investigate these two phenomena.

Model

Screw Body

The conduction model is formed by dividing the screw body (screw without flights) into domains according to shape of the root diameter, either a cylinder or a truncated cone (transition section). The use of spherical coordinates (see Appendix 1) provides precise modeling of the surface of the screw channel whether the section be cylindrical or conical.

Resin Temperature

The resin temperature must be calculated for the entire length of the screw to provide the temperature boundary condition for the screw body conduction model. Previously developed feed [1], melting [2], and pumping models [3,4] are used to calculate the resin temperature along the length of the screw in the channel.

Flights

The heat generated in the flight clearance will be conducted to the screw through the flights. The heat conduction in the screw flight is modeled as a fin [5] with heat transfer in the radial direction as shown in Appendix 2. Heat is transferred with the flight on either side and in the flight clearance. The melt in the flight clearance is modeled in detail [6] to include the heat generation there. An analytical solution for heat conduction in the flights for cylindrical coordinates is obtained.

Overall Screw Heat Balance

The resulting energy balance for the screw is made by coupling the feed, melting, pumping, and flight models

with the heat conduction model for the screw body proper similar to that previously done [7] for just the pumping section. Heat will be transferred with the screw such that the sum of all heat transferred equals the energy change of the screw. For steady-state operation the sum is zero, or the screw is operating autogenetically.

Extruder Scaling Effect

The model will now be used to calculate how extruder size (diameter) affects temperature. Four extruder diameters of 38.1 mm, 63.5 mm, 114.3 mm, and 203.2 mm are chosen. All screws are square pitched with a single flight and a 30:1 L/D ratio. Division of the length is 5D:3D:22D for feed, compression, and pumping sections. Pumping channel depths are 1.9, 2.54, 4.06, and 5.08 mm. Flight clearances are 0.0508, 0.0508, 0.203, and 0.508 mm. The compression ratio is 4.5:1 for all four screws.

The thermal conductivity of the metal is 17.6 J/s/m/K, and the specific heat is 1000 J/kg/K. The resin is HDPE, and its viscosity is modeled by the Carreau-Yasuda Equation. It is also assumed that the drive end of the screw requires that its temperature be held constant at 30°C.

The barrel zone temperature profiles are made nearly the same. The exception is the last two zones for the 38.1 and 63.5 mm extruders, which needed to be 325°C instead of 315°C to obtain the same product melt temperature as the two larger extruders. Individual screw speeds were then set to obtain the same exit melt temperature of 325°C for each extruder.

Figures 1-4 show the modeled temperature results for the four extruders at steady state. Values versus length are given for the

- 1) screw root temperature,
- 2) channel "melt" temperature,
- 3) barrel zone metal temperature,
- 4) flight tip temperature,
- 5) flight clearance melt temperature,
- 6) percent of solids, and
- 7) the root radius percent of barrel radius.

The screw root temperature follows the root surface of the screw in the axial direction. At the location of a flight, the temperature is that at the base of the flight where it joins the screw and not at the tip of the flight.

Interpretation of the "melt" temperature depends on the location in the extruder. In the feed portion, it is the solid feed resin temperature next to the barrel wall. In the melting portion, it is the average temperature in the channel

of the melted phase of the resin. In the pumping portion (fully melted), it is the average temperature of all of the resin in the channel.

Barrel zone temperatures refer to the metal at the surface of the bore. They are assumed to be held constant by controllers with heating or cooling as required.

The flight-tip and flight melt temperatures result from viscous heat generation in the flight clearance. The flight melt-temperature is the maximum temperature in the flight clearance, and it often is at the barrel-wall temperature. Flight tip and melt temperatures are shown as discrete points because they are not continuous in the axial direction. I.e., they follow a helical path and not an axial path.

The solids percentage is shown to indicate the beginning and ending of melting. The screw root percentage is based on the diameter of the extruder bore, and it serves to indicate the three sections of the screw.

Extruder Scaling Results

The screws are at a different temperature than the melt (or the barrel) as shown in Figures 1-4. Heat transfer between the resin and the screw generally occurs along most of the length of the extruder.

Temperature of the melt phase during melting is calculated to have a local maximum for all extruders. This maximum is lowest for the 38.1 mm extruder. The distance between melting and cooled drive end is less than 0.2 m for the 38.1 mm extruder, whereas it is progressively much longer for the larger extruders (up to 1.0 m for the 203.2 mm extruder). The short distance to the drive end for the 38.1 mm extruder requires a lower temperature difference to remove the heat from the melting process.

Of special interest is the action of the flights. They are shown to cause "spikes" in the screw root temperature. This is a result of the heat generation in the flight clearance. This heat is conducted radially to the screw root to locally raise its temperature.

However, the spikes can be pointed downward, which indicates that the flights are actually cooling the screw. In the melting portion of Figure 3, for instance, the barrel zone is much cooler than the melt-phase temperature so that the barrel is cooling the screw through the melt film in the flight clearance.

The flight melt-temperature and flight-tip temperature are nearly equal for the entire 38.1 mm 63.5 mm extruders (Figures 1 and 2). However, for the larger extruders (Figures 3 and 4), a difference between the flight melt-temperature and flight-tip temperature occurs. This is attributed to the larger flight clearance for the larger machines creating more resistance to heat flow. The clearances for the larger machines are 0.508 mm and 0.203 mm versus 0.0508 mm for the two smaller extruders.

Flight tip, flight melt, and average channel melt-temperatures all converge near the end of each extruder. However, the two larger extruders have an exit temperature about 10°C higher than the barrel metal, and the two smaller extruders have insignificant difference. This indicates that the smaller extruders produce the more uniform temperature profile at the exit.

Transient Results

The largest extruder (203.2 mm) is analyzed for the time needed for equilibrium after a speed change from 40 rpm to 80 rpm. Figure 6 shows the screw surface at ½-hour time intervals for the speed change. The model predicted that steady-state temperatures required about 2 hours for the speed change.

The model was used to predict the time for steady state for the other three extruders. In general, the time was proportional to the square of the extruder diameter (in proportion to screw mass/unit length of extruder). Time in hours for steady state conditions is then approximated by

$$\text{Time (hr)} = 50 [D \text{ (m)}]^2 \quad (1)$$

Experimental Verification

A 114.3 mm, 28:1 L/D extruder screw was used to obtain measured metal temperatures near the center of the screw. The screw had double flights with a lead of 139.7 mm. The metering depth was 3.17 mm and the compression ratio was 5. The screw configuration was 7D-4D-1.7D.

The screw was bored to about half of its length with a 25 mm diameter bore. A contact thermocouple was attached to a probe and then used to obtain metal temperatures of the bore surface at 6 equally spaced axial positions. Screw speed was 125 rpm and the polymer was LDPE. Figure 6 shows the results of the measured bore surface temperatures and the calculated results for the centerline of the screw. The data generally verify the model performance.

Also, the time for steady state to be reached during the experiments was measured, and this showed that equation 1 is an accurate conservative value of time for steady state to be reached.

Conclusions

1. The model of extrusion with heat conduction in the screw shows that the screw exchanges heat with the polymer under steady-state conditions. The screw is not generally adiabatic.
2. The size of the extruder is calculated to be an important factor in the axial temperature distribution in the screw.

3. Thermal transient times for speed changes depend on extruder size and are proportional to the square of the extruder diameter.

Nomenclature

a	Thermal diffusivity of screw metal
A_{CZ}	Area/unit screw length at screw root
C_1	Integration constant
C_2	Integration constant
C_3	Flight surface thermal constant
D	Extruder diameter
h_1	Heat transfer coefficient, flight wall
h_2	Heat transfer coefficient, flight wall
$I_0(mr)$	Bessel function of mr
$I_1(mr)$	Bessel function of mr
k	Screw thermal conductivity
k_m	Resin thermal conductivity
$K_0(mr)$	Bessel function of mr
$K_1(mr)$	Bessel function of mr
m	Bessel constant
q_{CZ}	Heat flux at the flight root
Q_{CZ}	Heat flow at the flight root
t	Time
T	Temperature in the solid
T_1	Resin temperature, left side of flight
T_2	Resin temperature, right side of flight
T_B	Barrel metal temperature
T_C	Flight temperature at root radius
T_F	Flight tip temperature
T_δ	Resin temperature in flight clearance
r	Spherical coordinate
r_c	Cylindrical coordinate
R	Extruder bore radius
R_C	Screw root radius
R_F	Flight radius
w	Flight width
z	Axial coordinate
δ	Flight clearance
Δz	Axial increment
$\Delta \chi$	Rotational increment
ϕ	Spherical coordinate
ϕ_F	Helix angle of the flight
χ	Rotational coordinate

Acknowledgement

The data of Figure 6 are the result of the experimental work of Mr. Barry George. His careful work is most appreciated.

References

1. Derezinski, S. J., "Control Volume Analysis of Extruder Feed Flow," Journal of Reinforced Plastics and Composites, Vol. 18, Number 5, 1999, pp 437-453.

2. Derezinski, S. J., "A Melting Rate Model Based on Extrusion Data," SPE ANTEC '99, Conference Proceedings, 1999, pp 184-189.

3. Derezinski, S. J., "Calculating Power of Extruder Melt Sections," Journal of Materials Processing & Manufacturing Science, Vol. 6, Number 1, July 1997, pp 71-77.

4. Derezinski, S. J., "Heat Transfer Coefficients in Extruder Melt Sections," SPE ANTEC '96, Conference Proceedings, 1996, pp 417-421.

5. Arpaci, V., Conduction Heat Transfer, Addison-Wesley Publishing Company, Reading, MA, 1966, pp 132-156.

6. Derezinski, S. J., "Calculating the Temperature in the Flight Clearance," SPE ANTEC '93, Conference Proceedings, 1993, pp 2243-2247.

7. Derezinski, S. J., "Developing Melt Temperature in Extruders Including Heat Transfer in the Screw," Journal of Plastic Film and Sheeting, Vol. 11, July, 1995, pp 204-215.

Appendix 1

Energy Equation for Conduction in the Screw

For conical screw sections (see Figure 7), the energy equation for spherical coordinates in two dimensions as a function of time is given as

$$\frac{1}{a} \frac{\partial T}{\partial t} = \frac{1}{r^2 \sin f} \frac{\partial}{\partial f} \left(\sin f \frac{\partial T}{\partial f} \right) + \frac{1}{r} \frac{\partial^2 (rT)}{\partial r^2} \quad (2)$$

For cylindrical sections all ϕ are zero, and

$$r \sin f = r_c, \quad (3)$$

$$r \partial f = \partial r_c, \text{ and} \quad (4)$$

$$\partial r = \partial z. \quad (5)$$

The spherical conduction equation becomes that for cylindrical coordinates as given by

$$\frac{1}{a} \frac{\partial T}{\partial t} = \frac{1}{r_c} \frac{\partial}{\partial r_c} \left(r_c \frac{\partial T}{\partial r_c} \right) + \frac{\partial^2 T}{\partial z^2} \quad (6)$$

A Runge-Kutta finite difference scheme is used to solve equations 2 and 6 for screw temperature as function of time and couple (equate) the solutions at the common boundaries between the sections.

The boundary conditions on the screw root are the temperatures given by the feed [1], melting [2], and pumping [3,4] models. However, at each flight root a heat flux boundary condition instead of temperature boundary condition is used. This is calculated by the following flight model in Appendix 2.

Appendix 2

Heat Conduction in a Flight

The equation for heat conduction for a fin in cylindrical coordinates [5] is used for the temperature of the flights as shown in Figure 7. The approximation is used that the area and perimeter of the flight (per unit length of screw) are proportional to the radial direction. The conduction in the flight is then given by

$$\frac{d}{dr_c} \left(r_c \frac{dT}{dr_c} \right) \quad (7)$$

$$-\frac{h_1 r_c}{wk} (T - T_1) - \frac{h_2 r_c}{wk} (T - T_2) = 0$$

subject to boundary conditions of

$$T(R_c) = T_c \quad \text{and} \quad (8)$$

$$k \frac{dT}{dr} = k_m \frac{dT_m}{dr} \quad \text{at} \quad (9)$$

$$R = R_F \quad (10)$$

The solution to equation 7 is

$$T = C_1 I_0(m r_c) + C_2 K_0(m r_c) + C_3 + T_1 \quad (11)$$

where

$$m = \sqrt{(h_1 + h_2) / (wk)} \quad (12)$$

and

$$C_3 = \frac{h_2}{h_1 + h_2} (T_2 - T_1) \quad (13)$$

The integration constants, C_1 and C_2 , are defined by the boundary conditions of equations 8 and 9 and the solution, equation 11 as

$$T_c = C_1 I_0(m R_c) + C_2 K_0(m R_c) + C_3 + T_1 \quad (14)$$

and

$$-k_m \frac{dT_d}{dr_c} = C_1 m I_1(m R_F) - C_2 m K_1(m R_F) \quad (15)$$

The temperature distribution of the melt in the flight clearance is numerically calculated [6] as a function of radius for the viscosity as a function of temperature and shear rate. The temperature solution is dependent on the boundary conditions of

$$T_d(R_F) = T_F \quad (16)$$

where

$$T_F = C_1 I_0(m R_F) + C_2 K_0(m R_F) + C_3 + T_1 \quad (17)$$

and

$$T_d(R) = T_B \quad (18)$$

The model provides the continuous temperature of the flight.

Heat transfer at the flight root is then given by

$$-k \frac{\partial T_c}{\partial r_c} A_{CZ} = Q_{CZ} = \quad (19)$$

$$[C_1 m I_1(m R_c) - C_2 m K_1(m R_c)] A_{CZ}$$

where flight root area is given as

$$A_{CZ} = w R_c \Delta z / (R_F \sin(\phi_F)) \quad (20)$$

The heat flux from the flight is calculated for the incremental surface area (see Figure 7) associated with the finite length of the finite difference solution as

$$q_{CZ} = \frac{Q_{CZ}}{\Delta z R_c \Delta C} \quad (21)$$

where

$$R_c \Delta C = \frac{\Delta z}{\tan(\phi_F)} \quad (22)$$

Equations 19-22 are combined to give the heat flux to the increment of screw length, which contains the flight as

$$q_{CZ} = -k \frac{\partial T_c}{\partial r_c} \frac{w R_c}{R_F \Delta z \cos(\phi_F)} \quad (23)$$

The assumption is made that the incremental length, Δz is larger than the axial flight dimension, $w / \cos(\phi_F)$.

38.1 mm, 250 rpm

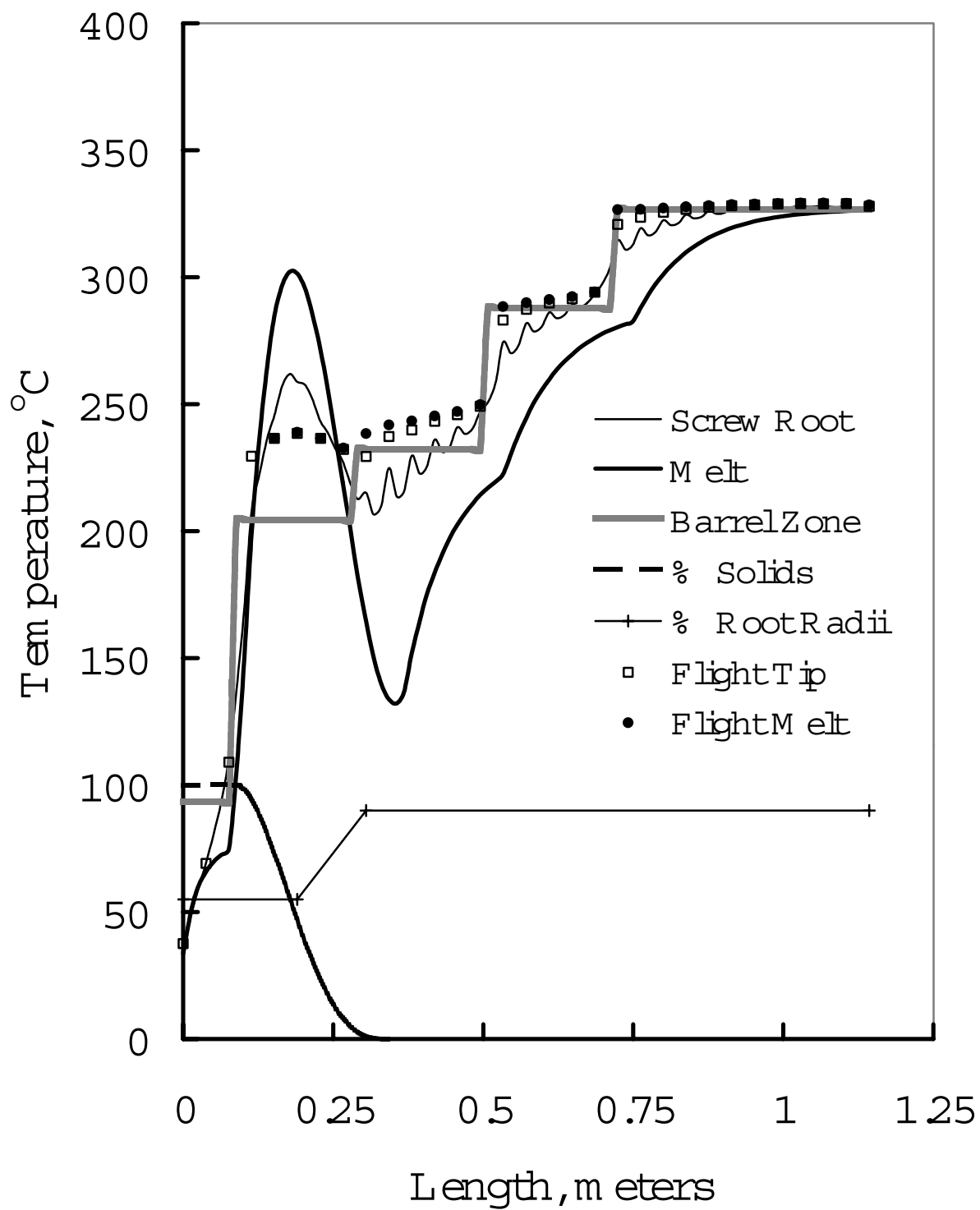


Figure 1. Steady-state temperature results for a 38.1 mm extruder.

63.5 mm, 200 rpm

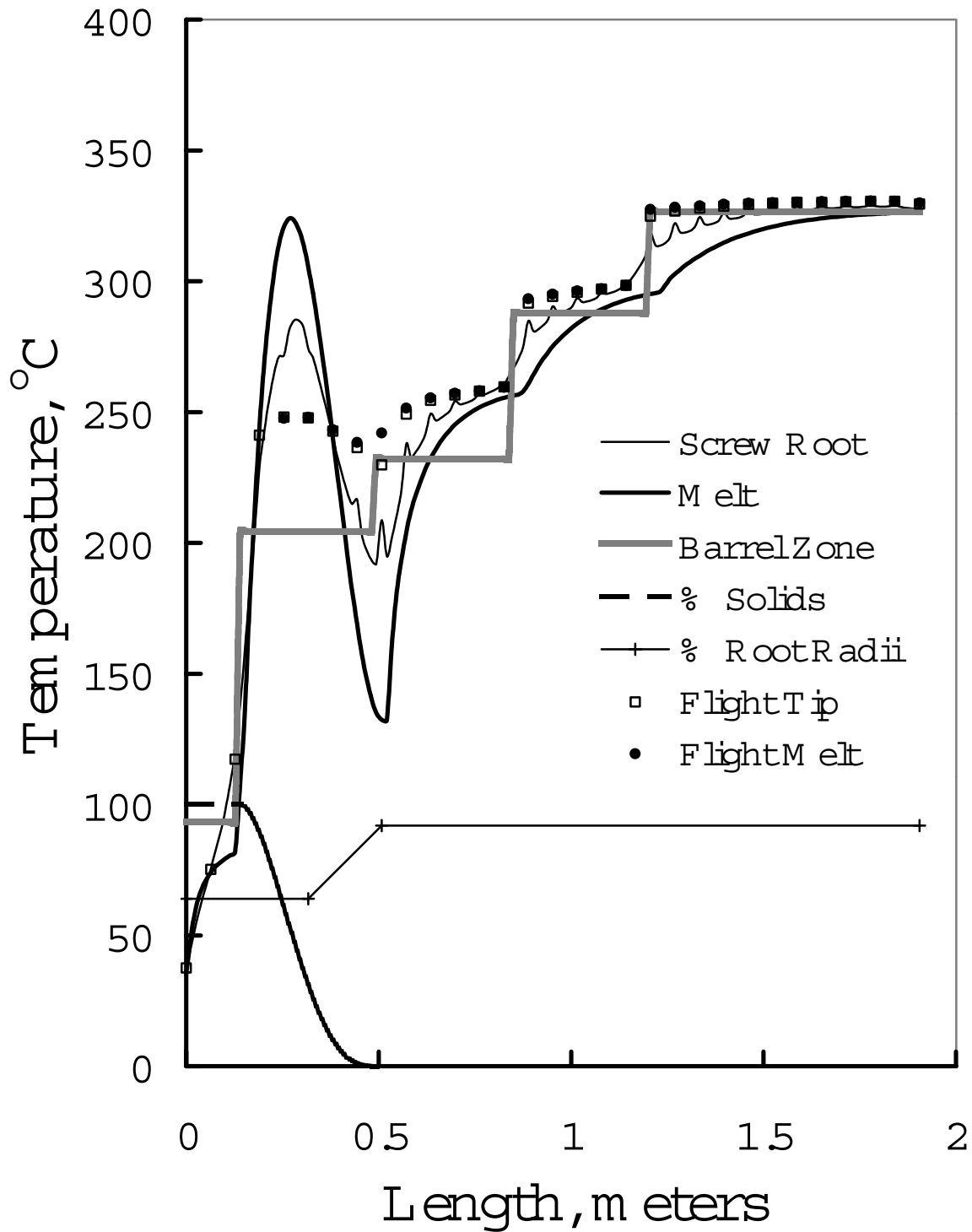


Figure 2. Steady-state temperature results for a 63.5 mm extruder.

114.3 mm, 150 rpm

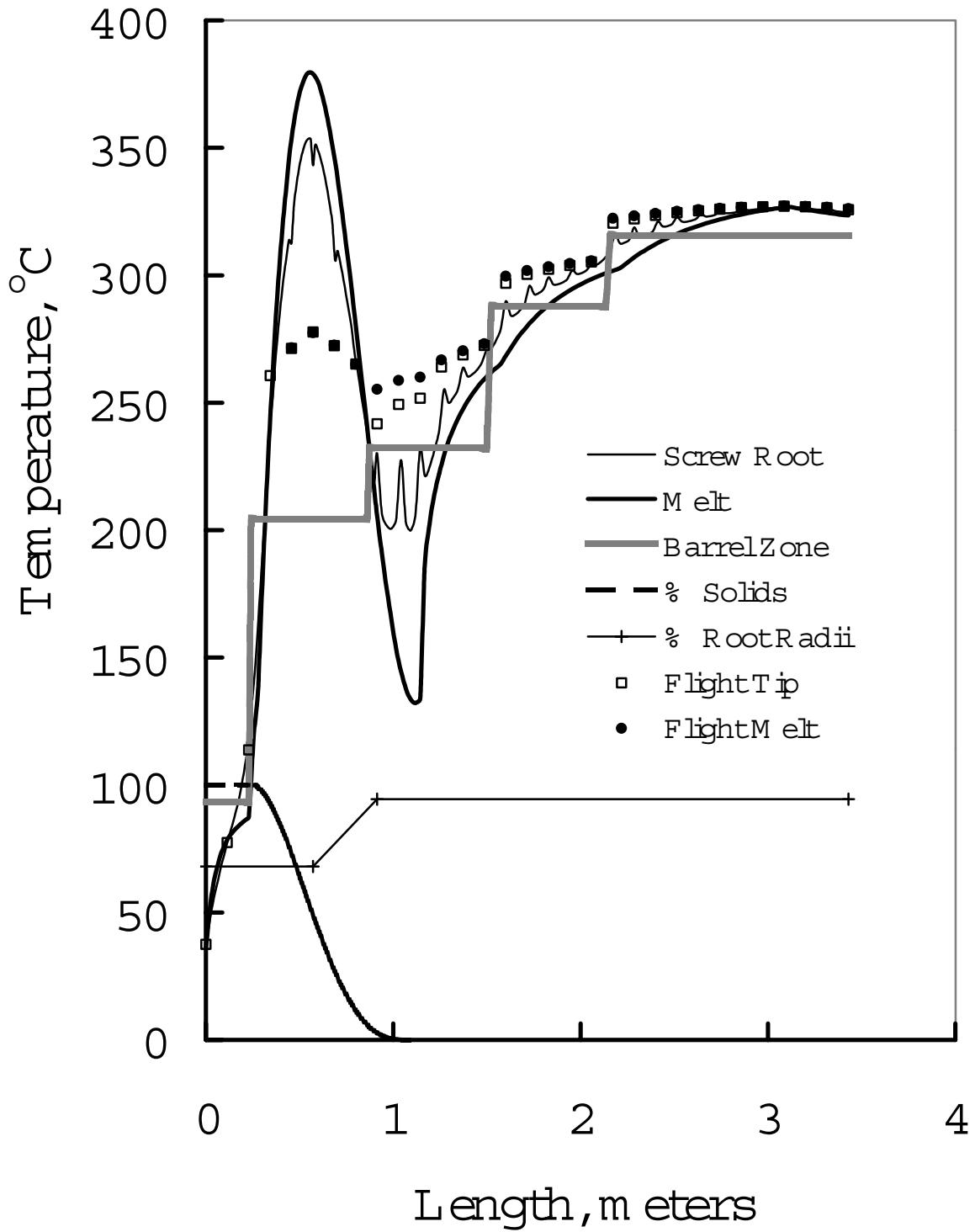


Figure 3. Steady-state temperature results for a 114.3 mm extruder.

203.2 mm, 80 rpm

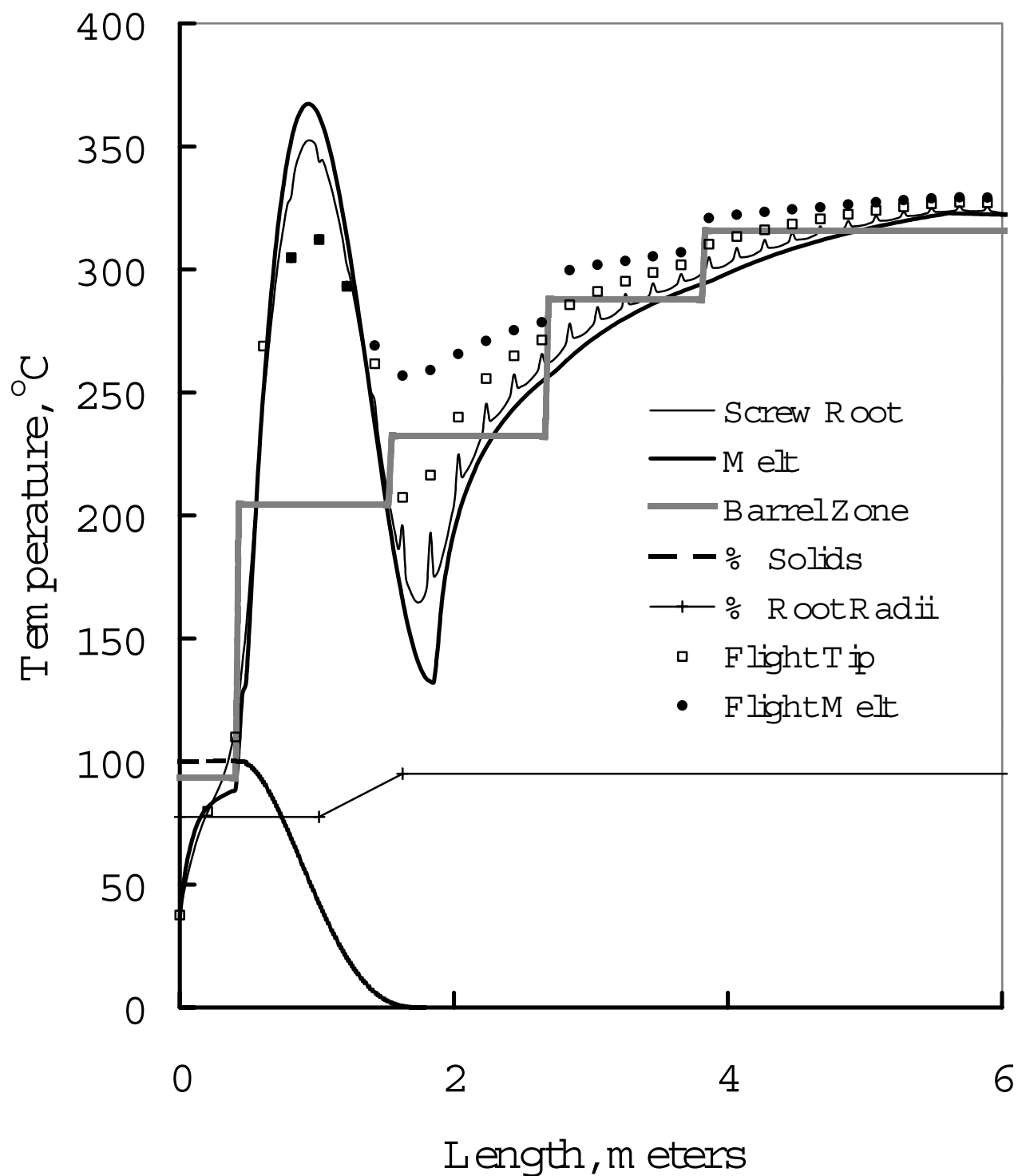


Figure 4. Steady-state temperature results for a 203.2 mm extruder.

203.2 mm SPEED CHANGE TRANSIENT

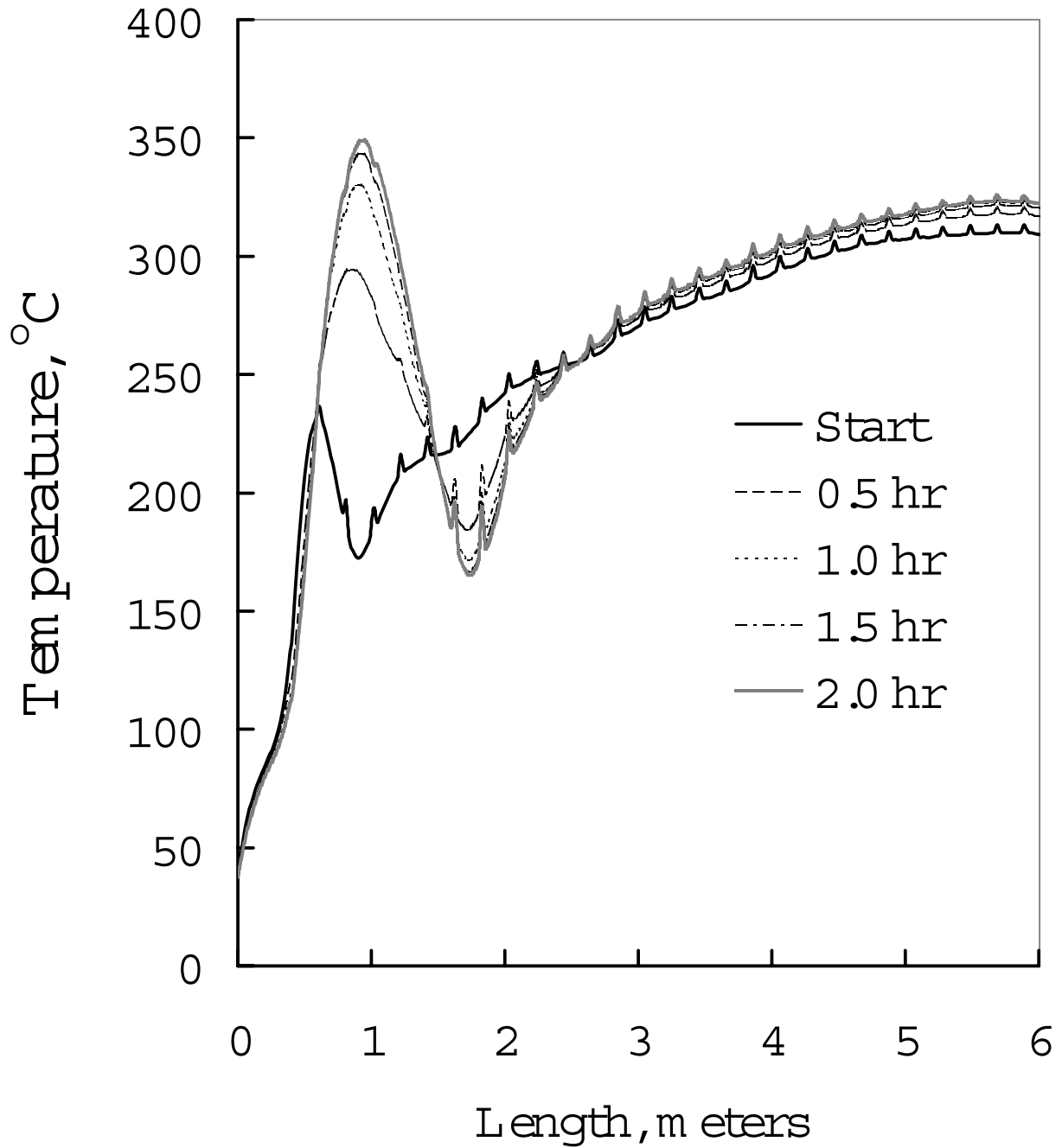


Figure 5. Extruder screw surface vs time. The screw speed at the start is 40 rpm. It is changed to 80 rpm and the surface temperature at 80 rpm is plotted at 0.5 hr intervals.

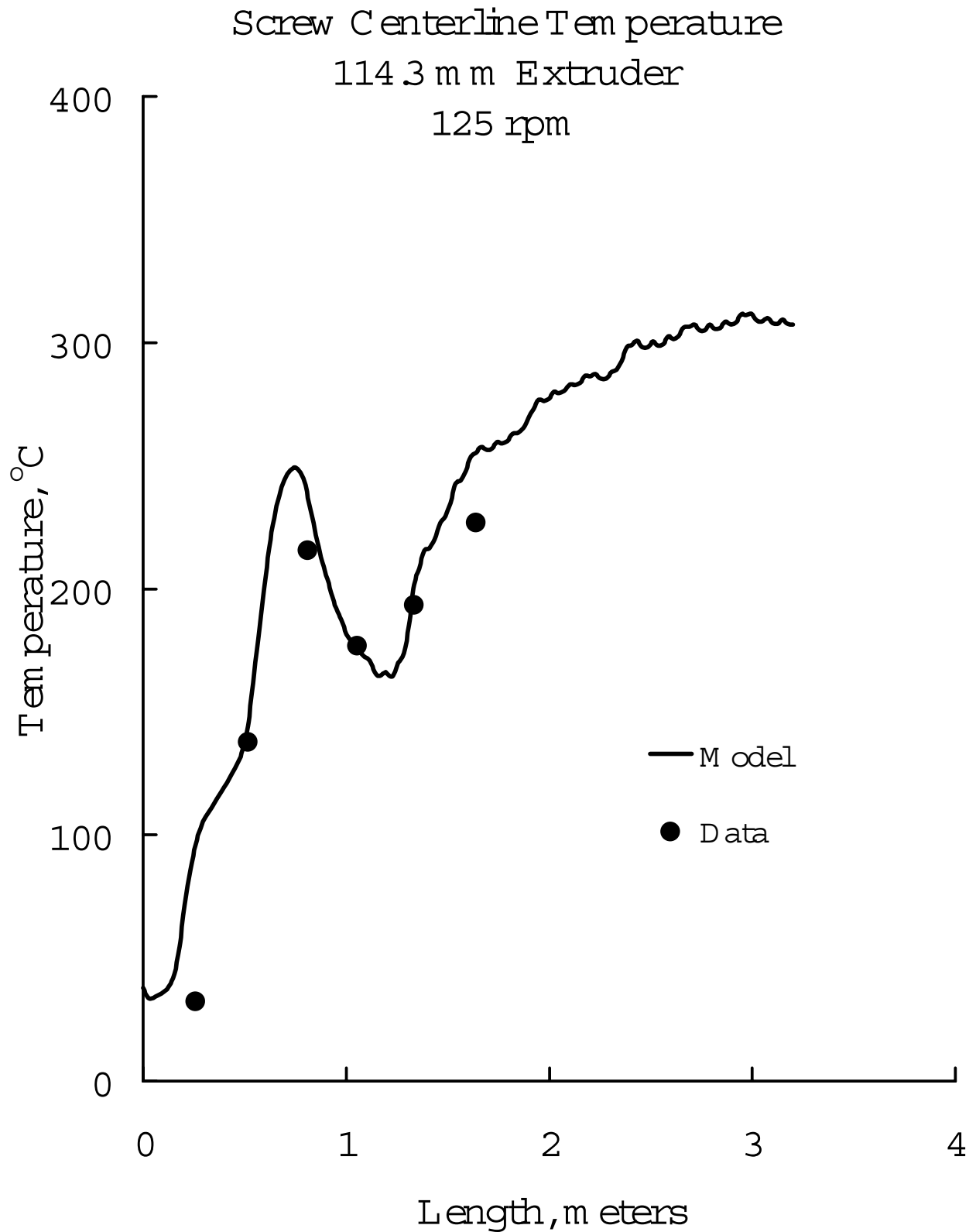
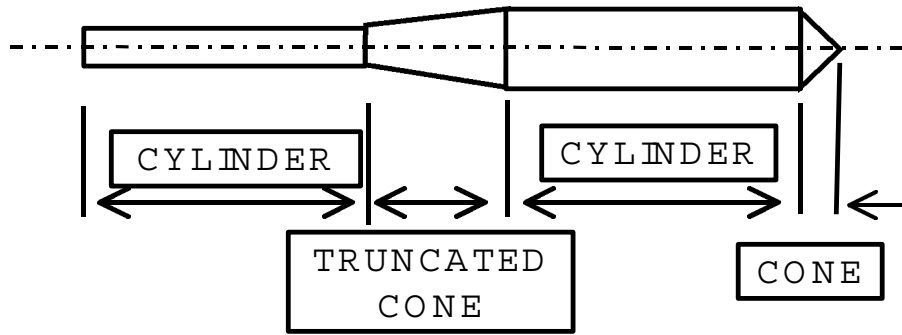
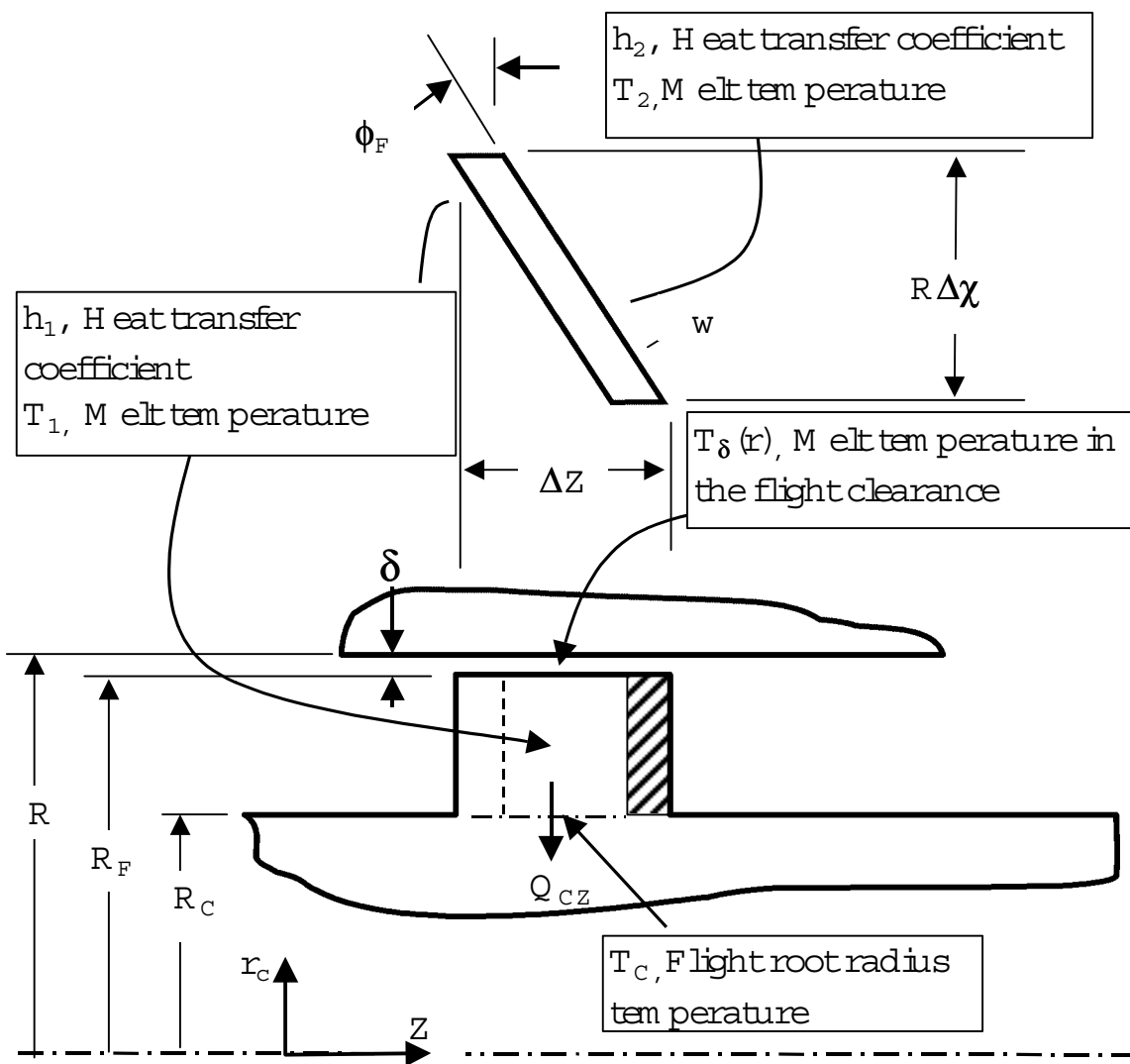


Figure 6. Centerline temperature of a 114.3 mm screw. Data are obtained from the surface of a 25 mm diameter bore in the screw. Screw configuration is 7D-4D-17D. CR is 5 with double flights.



Screw Conduction Model



Flight Conduction Model

Figure 7. The domains for the simulation of thermal conduction in the screw body and the geometry for the flight model.